ELSEVIER

Nuclear Physics A719 (2003) 177c–184c

NUCLEAR PHYSICS A

www.elsevier.com/locate/npe

Nuclear structure theory for the astrophysical rp-process and r-process

B. A. Brown[a], R. Clement[a], H. Schatz[a], J. Giansiracusa[a*], W. A. Richter[b], M. Hjorth-Jensen[c], K.-L. Kratz[d], B. Pfeiffer[d] and W. B. Walters[e]

[a]Department of Physics and Astronomy and National Superconducting Cyclotron Laboratory, Michigan State University, East Lansing, Michigan 48824-1321

[b]Department of Physics, University of Stellenbosch, Stellenbosch 7600, South Africa

[c]Department of Physics, University of Oslo, N-0316 Oslo, Norway

[d]Institute fur Kernchemie, Universitat Mainz, D-55128 Mainz, Germany

[e]Department of Chemistry, University of Maryland, College Park, Maryland 20742-2021

The astrophysical processes of rapid-proton capture and rapid-neutron capture require the knowledge of many nuclear properties which are not known from experiment. I will describe two examples of how theoretical models are used to provide this input. The first of these uses the Hartree-Fock method for displacement energies to obtain the masses of proton-rich nuclei needed for the rp-process. The second uses a model for configuration mixing near ^{132}Sn to provide Q values and beta-decay lifetimes for the r-process.

1. INTRODUCTION

There are a variety of theoretical tools which can be used for the calculation of nuclear-structure quantities which are needed for nuclear astrophysics. In this talk I will discuss ideas behind two rather different kinds of calculations. The first one for the rp-process uses Hartree-Fock results and is a summary of the theory used in a recently published paper [1]. The second one for the r-process is based upon shell-model configuration mixing for nuclei near ^{132}Sn. The methods and results for each these are discussed in the following two sections.

2. MASSES FOR THE rp-PROCESS

The masses for the proton-rich nuclei above $A = 60$ have not yet been measured. However, they are important for the astrophysical rp-process [2] which follows a path in nuclei near $N = Z$ for $A = 60 - 100$ [3]. In the absence of experimental masses for the proton-rich nuclei, one might use the masses based upon the Audi-Wapstra extrapolation (AWE) method [4]. However, one can obtain more accurate results by using the displacement energy systematics [5], [6], [7], [8]. The displacement energy is the difference in the binding

*Student from the University of Washington, Seattle who participated in the NSF sponsored Research Experience for Undergraduate Program at Michigan State University

0375-9474/03/$ – see front matter
doi:10.1016/S0375-9474(03)00914-X

energies of mirror nuclei for a given mass A and isospin T:

$$D(A,T) = BE(A,T_z^<) - BE(A,T_z^>), \tag{1}$$

where $T = \mid T_z^< \mid = \mid T_z^> \mid$, $BE(A,T_z^<)$ is the binding energy of the proton-rich nucleus and $BE(A,T_z^>)$ is the binding energy of the neutron-rich nucleus. The displacement energy can be more accurately calculated than the individual BE in a variety of models since it depends mainly on the Coulomb interaction. In particular, we will use the spherical Hartree-Fock model based upon the SKX set of Skyrme parameters [9], with the addition of charge-symmetry breaking (CSB), SKX_{csb} [10]. The CSB part of the interaction has one parameter which was adjusted to reproduce the displacement energies in the $A = 48$ mass region [11]. With the addition of CSB these calculations are able to reproduce the measured displacement energies for all but the lightest nuclei to within an rms deviation of about 100 keV [10]. In the $A = 40 - 76$ mass region the mass (binding energy) of most of the neutron-rich nuclei are experimentally usually known to within 100 keV or better. Thus we can combine the experimental binding energy for the neutron-rich nucleus $BE(T,T_z^>)_{exp}$ together with the Hartree-Fock value for $D(A,T)_{HF}$ to provide an extrapolation for the proton-rich binding energy:

$$BE(A,T_z^<) = D(A,T)_{HF} + BE(T,T_z^>)_{exp}. \tag{2}$$

The SKX_{csb} interaction is used to carry out Hartree-Fock calculations for all nuclei in the range $Z = 20 - 38$ and $N = 20 - 38$. The binding energies are then combined in pairs to obtain theoretical displacement energies for $A = 41 - 75$ and $T = 1/2$ to $T = 4$:

$$D(A,T)_{HF} = BE(A,T_z^<)_{HF} - BE(T,T_z^>)_{HF}. \tag{3}$$

The calculation is similar to those presented in [10], but as discussed in [1] several refinements are made, including a method for treating the "quasi-bound" states, and an exact-pairing model [12] for the nuclear and Coulomb interaction with $J = 0$ and $T = 1$. For the nuclei we considered, the occupation of the $g_{9/2}$ orbit is always small. It is known that deformed components of the 2s-1d-0g shell are essential for the nuclear ground states above $A = 76$ as indicated by the sudden drop in the energy of the 2^+ state from 709 keV in ^{72}Kr to 261 keV in ^{76}Sr. Thus we do not go higher than $A = 76$. In addition, one cannot always use Eq. (2) above $A = 76$ since many of the masses of the neutron-rich nuclei are not known experimentally. The results we obtain are not very sensitive to the exact distribution of the nucleons between the p and f orbits, since they have about the same rms radius and same single-particle Coulomb shift.

In Fig. 1 the calculated displacement energies (crosses) are shown in comparison with experiment (filled circles) in cases where both proton- and neutron-rich masses have been measured and with the AWE (squares) in cases where the mass of the proton-rich nucleus is based upon the AWE. The corresponding differences between experiment and theory are shown in Fig. 2 including the experimental or AWE error bars. It can be seen that when the displacement energy is measured the agreement with the calculation is excellent to within an rms of about 100 keV. The most exceptional deviation is that for $A = 54$ involving the ^{54}Ni-^{54}Fe mirror pair; a confirmation of the experimental mass for ^{54}Ni (which has a 50 keV error) would be worthwhile. The comparison based upon the AWE

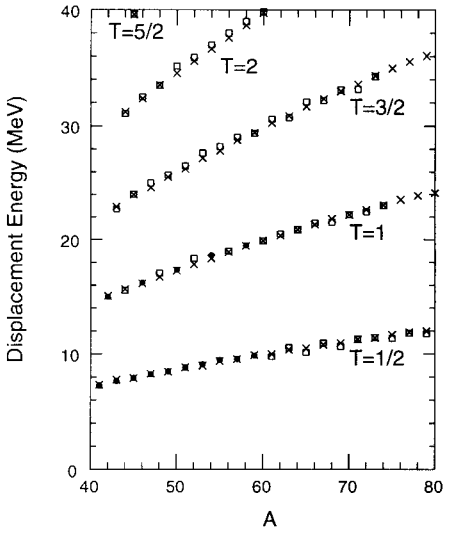

Figure 1. Calculated displacement energies (crosses) as a function of mass number. They are compared to experimental data (filled circles) and to values based upon the Audi-Wapstra extrapolations (squares).

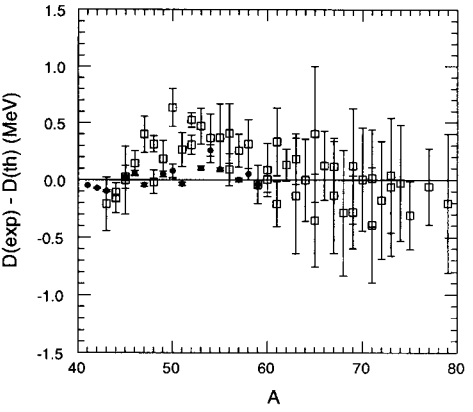

Figure 2. The difference between the calculated displacement energies and experiment (filled circles) or values based on the the Audi-Wapstra extrapolations (squares).

(squares) shows a much larger deviation with typically up to 500 keV differences, but the AWE error assumed is sometimes (but not always) large enough to account for the spread. The implication of this comparison is that the error in the HF extrapolation of the displacement energies is significantly less than the error in the AWE of the displacement energies.

The next step is to use Eq. (2) to calculate the binding energy of the proton-rich nuclei based upon the HF calculation of the displacement energy together with the experimental binding energy of the neutron-rich nucleus. The only neutron-rich nucleus whose mass is not yet experimentally measured is ^{71}Br for which we use the AWE value. The binding energies for the HF extrapolations for the proton-rich nuclei are given an error based upon the experimental error of the neutron-rich binding energy folded in quadrature with an assumed theoretical error of 100 keV for the displacement energy. This extrapolated set of binding energies for proton-rich nuclei together with the experimental binding energies for nuclei with $N = Z$ and neutron-rich nuclei provides a complete set of values from which the one- and two-proton separation energies are obtained. The masses for the $N = Z$ nuclei ^{66}As, ^{68}Se and ^{70}Br are not measured, and we use the AWE value.

Results for the one- and two-proton separation energies are shown in Fig. 3. The only nuclei in this figure for which masses have been measured are those with a line in the lower

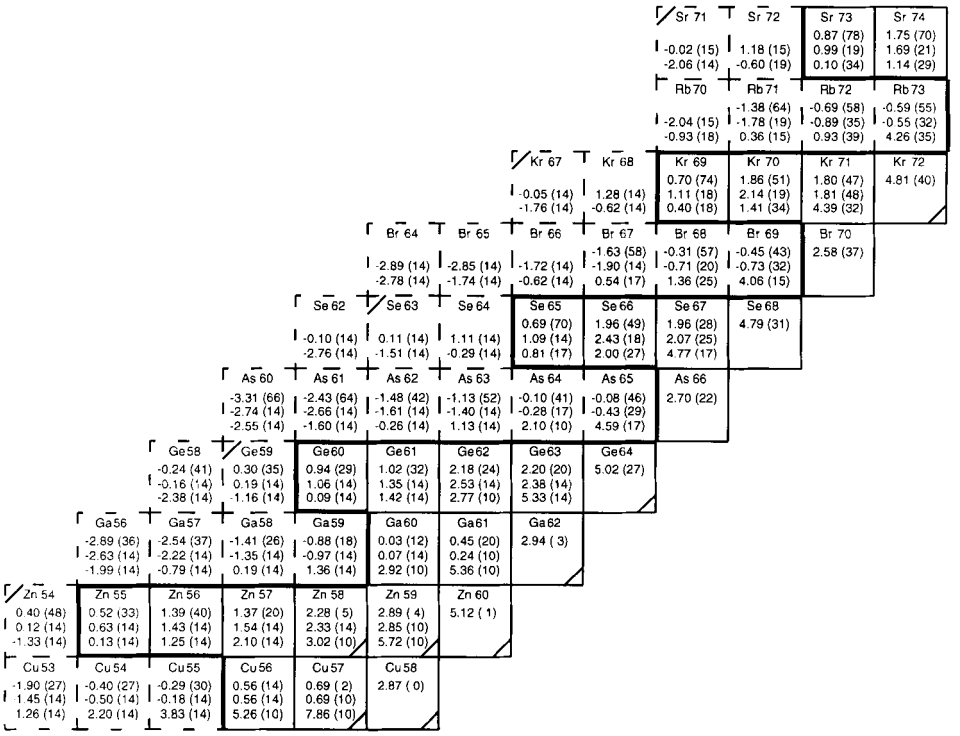

Figure 3. A section of the mass chart for $N = Z$ and proton-rich nuclei. See the text for a discussion.

right-hand corner. The first number in each box is the one-proton separation energy based upon the AWE with the associated error. The second number is the one-proton separation energy based upon the present HF extrapolation, and the third number is the two-proton separation energy based upon the HF extrapolation. The error in the separation energies is the error for the binding energies of the parent and daughter nuclei folded in quadrature.

The double line in Fig. 3 is the proton-drip line beyond which the one-proton separation energy and/or the two-proton separation energy becomes negative. However, due to the Coulomb barrier, some of the nuclei outside the proton-drip line may have lifetimes which are long enough to be able to observe the nuclei in radioactive beam experiments. The observation of ^{64}As and ^{65}As in the experiment of Blank et al. [13] excludes half-lives which are much shorter than 1 μs which indicates that they are unbound by less than 400 keV. This is compatible (within error) with the HF results given in Fig. 3. The non-observation of ^{69}Br in the radioactive beam experiment of Pfaff et al. [14] means that its lifetime is less than 24 nsec which implies that it is proton unbound by more than 500 keV [14]. This is also compatible with the HF result shown in Fig. 3. The non-observation of

^{73}Rb in the experiment of Janas et al. [15] gives an upper limit of 30 nsec for the half-life which implies that ^{73}Br is proton unbound by more than 570 keV, again in agreement (within error) of the present HF result. Thus all of the current experimental data are consistent with our calculations. The most promising candidates for the illusive diproton emission are indicated by a line in the upper left-hand corner.

These present masses have been used in a one-dimensional, one-zone x-ray burst model in order to see the implications for the time scale for the rp-process and the resulting nuclear abundances. The details of this calculation and the results are discussed in [2]. The results is that the end products are more tightly constrained compared to those obtained from the AWE model. Most of the remaining uncertainty for the rp-process comes from a few key "waiting point" nuclei with $N = Z$ (for which the displacement energy method cannot be applied) that have relatively large experimental or extrapolated errors. In particular, the masses of ^{68}Se and ^{64}Ge need to be measured to within an accuracy of about 50 keV or better. Other key nuclei whose mass measurements will test the present method and improve the rp-process results are given in Table II of [1].

3. CONFIGURATION MIXING FOR THE r-PROCESS

The region of nuclei around the neutron-rich nucleus ^{132}Sn is an active area of experimental and theoretical investigation. ^{132}Sn is one of the best magic nuclei. New experimental results on the single-particle properties in nuclei with one nucleon added or removed form ^{132}Sn enable quantitative shell-model calculations to be carried configurations in nuclei further removed from ^{132}Sn. The properties of nuclei in this region is of prime importance for the position of the r-process path which determines the r-process element abundance.

We have carried out shell-model configuration-mixing calculations based upon a modern renormalized G matrix residual interaction in a model space which can incorporate all nuclei around ^{132}Sn. For the application to the r-process we have considered the binding energy, level structure and Gamow-Teller beta decay of nuclei near $N = 82$ below ^{132}Sn. Calculations by other groups for the the beta decay of the neutron-rich $N = 82$ isotones are given in [16] and [17].

These nuclei have been recognized for their importance in the astrophysical rapid neutron-capture process (r-process) [18], in which a strong neutron flux causes seed nuclei to capture neutrons, pushing mass far from the valley of stability and into the neutron rich unstable region. Mass moves quickly along the r-process path, guided by the competing processes of neutron capture and β-decay, until it reaches the shell closure at $N = 82$ where the decreased neutron separation energies prevent the further capture of neutrons. At this point the mass accumulates in these $N = 82$ isotones, where it climbs to higher charge number as each β-decay allows another capture. The ascent is slowed as the β half-lives extend. The nuclei ^{129}Ag and ^{130}Cd, with their longer half-lives, become waiting points in the process. When the neutron flux ceases (it is estimated to extend for a period on the order of seconds), the distribution of mass in these waiting point nuclei decays towards the valley of stability, producing elemental abundance spectrum observed in the universe. The properties of these waiting-point nuclei are particularly sensitive parameters in the results for r-process nucleosynthesis [19]. The predictions made here go

towards predicting the half-lives of these as well as many other nuclei involved.

The calculations were carried out in the proton-neutron formalism with the shell-model code OXBASH. The model space consists of 20 orbitals in the four major shell surrounding ^{132}Sn. Most of the calculations were obtained in a truncation in which ^{132}Sn is a closed shell. In the simplest model we take ^{132}Sn as a closed shell. But, the model space and hamiltonian can also be applied to open-shell configurations in ^{132}Sn (particle-hole excitations across the closed shell), and this is necessary for the beta decay of nuclei with $Z \leq 50$ and $N > 82$.

For the r-process results discussed here we only use the model space with (A) four proton-hole orbits ($0f_{5/2}$, $1p_{3/2}$, $1p_{1/2}$, and $0g_{9/2}$) and (B) five neutron-hole orbits ($0g_{7/2}$, $1d_{5/2}$, $1d_{3/2}$, $2s_{1/2}$, and $0h_{11/2}$). Most of the single-particle energies (SPE) can be obtained from the experimental binding energy and levels schemes for ^{131}Sn and ^{131}In [20] to within an error of about 100 keV. The $1p_{3/2}$ and $0f_{5/2}$ hole states in ^{131}Cd have not yet been observed. The $1p_{3/2}$ SPE was obtained from the $1p_{3/2}$-$1p_{1/2}$ spin-orbit splitting obtained in the SKX [11] Skyrme Hartree-Fock model and the $0f_{5/2}$ SPE is that given the the SKX model. It has been suggested [21], [22] that the position of the $11/2^-$ state in ^{131}Sn may have a larger uncertainty than indicated in the literature [20], but a few hundred keV shift of this level does not greatly change the results discussed below.

The residual two-body interaction is obtained starting with a G-matrix derived from the CD-Bonn [23] nucleon-nucleon interaction. A harmonic oscillator basis was employed for the single-particle wave functions with an oscillator energy $\hbar\omega$=7.87 MeV. The G-matrix elements form in turn the starting point for a perturbative derivation of a shell-model effective interaction. In this work we derive the effective interaction for the above shell-model space by the $\hat{Q}$-box method which includes all so-called non-folded diagrams through third-order in the interaction G and sums up the folded diagrams to infinite order [24]. This type of hamiltonian has been used to describe spectra of tin isotopes from mass number $A = 102$ to $A = 130$ [25] and the $N = 82$ isotones up to $A = 146$ [26] with good agreement with data. For the protons, we also add the Coulomb interaction calculated with the same harmonic-oscillator energy.

In the truncation in which ^{132}Sn is a closed shell, there is only one allowed single-particle transition for Gamow-Teller (GT) beta decay: $\nu 0g_{7/2} \rightarrow \pi 0g_{9/2}$. The value of the effective single-particle matrix element for this transition was adjusted to reproduce the B(GT) value for the ^{131}In $\rightarrow$ ^{131}Sn decay which is just a single-particle transition relative to the ^{132}Sn closed shell this simplest model. In terms of the filled shells A and B, this single-particle transition has the form $A^{(-1)}B \rightarrow AB^{(-1)}$. The value of the effective single-particle matrix element is about a factor of three smaller than its (free-nucleon) single-particle value. This GT transition considered within the model space is only one of many which contribute to the full GT strength corresponding to transitions to neutron-particle states above ^{132}Sn. For the ^{131}In decay we can enlarge the model space to include these neutron-particle states. We find that a small mixture of these "giant GT" states are responsible for most of the reduction in the effective $\nu 0g_{7/2} \rightarrow \pi 0g_{9/2}$ matrix element. The remaining part of the reduction may come from higher-order configuration mixing and mixing with delta-nucleon-hole configurations as found for light nuclei [27]. Since the giant GT mixture is only a small part of the wave function, it is reasonable to assume that its effect is perturbative. Thus, in order to continue the calculations down to ^{122}Zn, we treat

^{132}Sn as a closed shell and take a constant effective matrix element for $\nu 0g_{7/2} \rightarrow \pi 0g_{9/2}$. We assume that the beta decay for $N \leq 82$ is dominated by the Gamow-Teller transition. More complete calculations which include first-forbidden contributions will have to wait for a future work.

The results of our approach has recently been tested against new data obtained for the decay of ^{130}Cd to ^{130}In [28]. In our model space ^{130}Cd GT decays to only one 1^+ state in ^{130}In. The interpretation of the experimental data is that about 80% of the decay does go to a single 1^+ state with a $B(GT)$ value of about 0.25(5) compared with the calculated value of 0.25. However, the experimental energy of the 1^+ state is suggested to be at 2.12 MeV compared to our predicted energy of 1.38 MeV. Our calculations based on the G matrix interaction for the $T = 1$ spectra in nuclei such as ^{130}Sn [25], ^{134}Te [26] and ^{134}Sn [29] agree with experiment to within an rms of about 100 keV. Thus, this large difference for the 1^+ energy in ^{130}In is surprising, although this $T = 0$ part of the interaction is previously not so well tested. In particular, the two-body matrix element (TBME) $< 0g_{9/2}, 0g_{7/2}, 1^+ \mid V_{pn} \mid 0g_{9/2}, 0g_{7/2}, 1^+ > = -2.8$ MeV is the largest proton-neutron TBME in the model space. To improve agreement with experiment we would need to change ("renormalize") this TBME to about -2.0 MeV. It is not clear why this happens. Since the G matrix is obtained with harmonic-oscillator radial wave functions which are the same for protons and neutrons, we may expect some overlap correction in a finite-well potential. But this correction should only be on the order of 10%.

We have calculated the binding-energy and decay properties of other nuclei near $N = 82$ down to ^{122}Zr. A typical set of half-lives (in ms) obtained for $N = 82$ is 180 (^{130}Cd), 68 (^{129}Ag), 44 (^{128}Pd), 25 (^{127}Rh), 16 (^{126}Ru), 14 (^{125}Tc), 7 (^{124}Mo), 7 (^{123}Nb) and 4 (^{122}Zr). Below ^{130}Cd the GT strength in our calculation become fragmented into many final state some of which are unbound to neutron decay. Generally these neutron decay branches are large for the odd-even $N = 82$ nuclei. We have used these values (together with the calculated one-neutron separation energies) in a typical r-process scenario. The resulting r-process element abundance for $A = 126 - 128$ is too small relative to $A = 129 - 132$ compared to solar abundance. There may perhaps be astrophysical reasons for this beyond what is already in the models. But from the nuclear structure side we will need to have a deeper understanding of the defects in the hamiltonian (and perhaps model space) in order to have more confidence in the results.

Acknowledgements

Support for this work was provided from US National Science Foundation grant number PHY-0070911.

REFERENCES

1. B. A. Brown, *et al.*, Phys. Rev. C 65 (2002) 045802.
2. R. K. Wallace and S. E. Woosley, Astrophys. J. 45 (1981) 389.
3. H. Schatz *et al.*, Physics Reports 294 (1997) 167.
4. G. Audi, A. H. Wapstra, Nuclear Physics A 595 (1995) 409.
5. B. A. Brown, Phys. Rev. C 42 (1991) R1513.
6. W. E. Ormand, Phys. Rev. C 53 (1996) 214.

7. W. E. Ormand, Phys. Rev. C 55 (1997) 2407.
8. B. J. Cole, Phys. Rev. C 54 (1996) 1240.
9. B. A. Brown, Phys. Rev. C 58 (1998) 220.
10. B. A. Brown, W. A. Richter and R. Lindsay, Phys. Lett. B 483 (2000) 49.
11. B. A. Brown, Phys. Rev. C 58 (1998) 220.
12. A. Volya, B. A. Brown and V. Zelevinsky, Phys. Lett. B 509 (2001) 37.
13. B. Blank *et al.*, Phys. Rev. Lett. 74 (1995) 4611.
14. R. Pfaff *et al.*, Phys. Rev. C 53 (1996) 1753.
15. Z. Janas *et al.*, Phys. Rev. Lett. 82 (1999) 295.
16. G. Martinez-Pinedo, and K. Langanke, Phys. Rev. 83 (1999) 4502.
17. J. Engle, *et al.*, Phys. Rev. C 60 (1999) 014302.
18. E. M. Burbridge *et al.*, Rev. Mod. Phys. 29 (1957) 547.
19. B. Pfeiffer *et al.*, Nucl. Phys. A 693 (2001) 282.
20. R. B. Firestone, *et al.*, Table of Isotopes, Eighth Edition (Wiley Interscience, 1996).
21. J. Genevey *et al.*, Eur. Phys. J. A 7 (2000) 463.
22. H. Mach, private communication.
23. R. Machleidt, F. Sammarruca and Y. Song, Phys. Rev. C 53 (1996) R1483.
24. M. Hjorth-Jensen, T. T. S. Kuo and E. Osnes, Phys. Reports 261 125 (1995); M. Hjorth-Jensen, H. Muther, E. Osnes and A. Polls, J. Phys. G 22 (1996) 321.
25. A. Holt, T. Engeland, M. Hjorth-Jensen, and E. Osnes, Nucl. Phys. A 634 (1998) 41.
26. A. Holt, *et al.*, Nucl. Phys. A 618 (1997) 107.
27. B. A. Brown and B. H. Widlenthal, Phys. Rev. C 28 (1983) 2397.
28. I. Dillmann and K.-L. Kratz *et al.*, Proceedings of the CGS11 Conference, Pruhonice Czech Republic, September 2002 (World Scientific, to be published).
29. B. Fornal *et al.*, Phys. Rev. C 63 (2001) 024322.